American Mineralogist, Volume 73, pages 1405–1419, 1988

Chemistry and radiation effects of thorite-group minerals from the Harding pegmatite, Taos County, New Mexico

GREGORY R. LUMPKIN, B. C. CHAKOUMAKOS
Department of Geology, University of New Mexico, Albuquerque, New Mexico 87131, U.S.A.

ABSTRACT

Dark brown and yellow thorites, with compositions extending the range of natural solid solution for the zircon structure type, occur as 0.5- to 2-cm grains in the quartz zone, cleavelandite unit (replacing the beryl zone), quartz–lath spodumene zone, and microcline-spodumene zone of the Harding pegmatite, Taos County, New Mexico. Electron-microprobe analyses (wt%) give the following for thorites from the cleavelandite unit: 2.9–19.6 P_2O_5, 6.4–16.5 V_2O_5, 0.2–1.2 As_2O_5, 2.6–7.7 SiO_2, 41–57 ThO_2, 0.0–0.9 UO_2, 0.1–2.9 Y_2O_3, 0.1–6.5 REE_2O_3, 0.0–4.7 Bi_2O_3, 5.8–8.4 CaO, 0.1–0.6 PbO, and 0.4–1.7 F. In contrast, yellow thorites from the quartz zone contain (wt%) 17–20 SiO_2, 36–65 ThO_2, 3–20 UO_2, 0.4–0.8 Al_2O_3, 0.3–0.6 Y_2O_3, 0.2–0.6 REE_2O_3, 0.6–1.0 Bi_2O_3, 0.8–1.3 CaO, 3–17 PbO, and 0.0–0.9 F. Low totals of the microprobe analyses probably indicate the presence of 7–12 wt% H_2O, in agreement with TGA. Infrared spectra confirm the presence of molecular water and are consistent with the presence of mixed types of hydroxyl species. Both varieties of thorite are partially recrystallized. In the brown variety, the degree of crystallinity correlates with increasing substitution of P, V, and Ca for Si and Th.

Dark brown thorites from the quartz-lath spodumene zone have an average composition near $(Th_{0.87}U_{0.08}Pb_{0.05})SiO_4$, are fully metamict, and show only slight alteration. Thorites from a partially albitized area of the microcline-spodumene zone show slight to moderate alteration characterized by enrichment in P, V, As, and Ca. Compositions (wt%) are 0.2–7.0 P_2O_5, 0.2–6.0 V_2O_5, 0.1–1.8 As_2O_5, 7.8–19.4 SiO_2, 0.3–2.6 ZrO_2, 61–75 ThO_2, 0.7–3.5 UO_2, 0.1–0.9 Al_2O_3, 0.1–0.4 REE_2O_3, 1.9–4.5 CaO, 0.1–0.5 PbO, and 0.2–0.9 F. Altered areas are partially recrystallized.

Calculated alpha-event doses ($4–12 \times 10^{17}$ α/mg) are greater than the damage saturation dose ($\sim 1 \times 10^{16}$ α/mg), but substantial crystallinity is present. The energy barrier to recrystallization of alpha-decay–damaged thorite enriched in P and V is inferred to be lower than for ideal thorite or U-rich microlites from the microcline-spodumene zone.

Thorite from the quartz, quartz–lath spodumene, and microcline-spodumene zones crystallized as a primary magmatic phase close in composition to ideal thorite, but enriched in U. Partial alteration of primary thorite in the microcline-spodumene zone is related to partial replacement of this unit by cleavelandite. Brown thorites also crystallized during subsolidus replacement of the beryl zone by cleavelandite. The hydrothermal fluid present during albitization of the beryl zone and microcline-spodumene zone was enriched in Ca, V, P, As, Y, REEs, and Bi. U was depleted by the earlier formation of microlite in the quartz–lath spodumene and microcline-spodumene zones. Remaining U was preferentially incorporated by microlite in the cleavelandite unit. Thorite concentrated Y, REEs, and Bi relative to microlite.

INTRODUCTION

In 1928, Hirschi published a brief description of an unnamed mineral containing 32.35 wt% Th and 0.185 wt% U from the Harding pegmatite, Taos County, New Mexico. Discussion and a partial translation of Hirschi's description appeared in Northrop (1959), but no name was assigned or further description made. To our knowledge, none of these samples was preserved. Recently, Arthur Montgomery collected and donated to us two samples from the Harding pegmatite that contained an unidentified ochre-colored mineral. These samples appear to be similar to those described by Hirschi (1928), although the paragenesis is not exactly the same as noted in the original description.

During field investigations we have found additional samples of dark brown, brown, and yellow material in the beryl zone, quartz zone, quartz–lath spodumene zone, and microcline-spodumene zone. Preliminary work showed that all of the samples possess the zircon structure ($I4_1/amd$, Z = 4) with lattice constants similar to ideal

0003–004X/88/1112–1405$02.00

thorite (Lumpkin and Chakoumakos, 1986). Chemical compositions of the samples are complex, ranging from U-Pb–rich thorite to varieties in which the components $CaTh(VO_4)_2$ or $CaTh(PO_4)_2$ predominate. Furthermore, rare-earth elements (REEs), Bi, and F were detected by electron-microprobe analysis.

Other species with the zircon structure in which B = V are wakefieldite, YVO_4 (Hogarth and Miles, 1969; Miles et al., 1971), and dreyerite, $BiVO_4$ (Dreyer and Tillmanns, 1981). The only naturally occurring orthophosphate with the zircon structure is xenotime, YPO_4. Brabantite, near–end member $CaTh(PO_4)_2$, has the monazite structure as do the synthetic Sr and Pb analogues (Rose, 1980). Natural $ThSiO_4$ occurs as the polymorphs thorite and huttonite, which has the monazite structure (Pabst and Hutton, 1951; Taylor and Ewing, 1978; Speer, 1982). Previous work has shown that thorite can contain (wt%) up to 20 UO_2, 15 REE_2O_3, 6.3 Y_2O_3, 4.8 ZrO_2, 5.8 CaO, 4.0 P_2O_5, and 2.1 As_2O_5 (Frondel, 1953; Robinson and Abbey, 1957; Staatz et al., 1976; Speer, 1982). For most thorites, analytical data have been obtained by wet-chemical methods on impure material, hindering the calculation of empirical formulas. To complicate matters, water is usually present at 5–16 wt%. As in zircon, the problem arises as to whether the water occurs as OH^- or H_2O (cf. Speer, 1982).

The major naturally occurring ABO_4 structure types include monazite, zircon, fergusonite, and scheelite. At given values of temprature and pressure, stability fields of the different structure types can be delineated in terms of the ionic radii of the A and B cations (Muller and Roy, 1974; Aldred, 1984). In nature, monazite, huttonite, and xenotime are invariably crystalline, whereas zircon, thorite, and fergusonite often occur in the metamict state, amorphous to x-ray and electron diffraction (Palache et al., 1944; Pabst, 1952; Frondel, 1958; Mitchell, 1973; Ewing, 1975; Ewing and Haaker, 1980). Such observations suggest that in addition to annealing kinetics, both structure and composition affect the ability of a particular phase to sustain alpha-recoil damage (Ewing and Haaker, 1980). Thorite appears to be particularly susceptible to low-temperature alteration and annealing to secondary, hydrated thorite (Frondel, 1953; Robinson and Abbey, 1957). An important aspect of this work involves the study of radiation effects in thorite using X-ray diffraction and transmission electron microscopy. Results are applicable to the study of long-term stability relations in crystalline nuclear waste forms and to the geochemistry of radiogenic elements commonly used for age dating. Furthermore, detailed chemical data allow for an interpretation of the behavior of rare elements during pegmatite emplacement.

Experimental details

Electron-microprobe analysis

Chemical analyses were obtained using a JEOL733 Superprobe operated at 15 kV and 20 nA and using a 10-μm beam. Each element was counted for a maximum of 20 s or until a standard deviation of 0.5% was reached on the accumulated number of counts. Data were reduced following the empirical alpha-factor approach developed by Bence and Albee (1968) and Albee and Ray (1970). Standards for data reduction were $ThSiO_4$ (Th, Si), UO_2 (U), YPO_4 (Y), $REEPO_4$ (La, Ce, Nd, Sm, Gd, Dy, Er, Yb), $ZrSiO_4$ (Zr), $NaNbO_3$ (Na), apatite (Ca, P, F), vanadinite (Pb, V, Cl), mimetite (As), olivine (Mg, Fe), stibiotantalite (Sb, Bi), manganotantalite (Mn), and anorthite (Al).

Infrared spectroscopy

Infrared spectra were recorded with a Nicolet model 6000 FT-IR spectrometer. Data were collected over the range 400–4000 cm^{-1} at room temperature. Samples were in the form of pressed pellets consisting of a finely ground mixture of ~300 mg of KBr and ~0.5 mg of thorite.

Thermogravimetric analysis

Weight-loss measurements were made on powdered aliquots of two samples using a DuPont model 951 TGA and model 990 recorder. Samples weighing 10–20 mg were heated in air from room temperature (~25 °C) to 1000 °C at a rate of 10 °C/min. The instrument was calibrated using calcium oxalate as a standard.

Transmission electron microscopy

Crushed grains of sample HT5 were deposited onto a holey C film supported by a 200 mesh Cu grid. Thin edges of grains were examined with a JEOL 2000FX transmission electron microscope operated at 200 kV. Electron-diffraction patterns were calibrated using a polycrystalline Au film. High-resolution images were taken at 500 000× using axial illumination and a 100-μm objective lens aperture. Images were calibrated using a partially graphitized carbon-black standard.

X-ray diffraction analysis

Powdered aliquots of three samples were deposited on polished quartz (low background) slides and scanned from 5 to 85° 2θ using a SCINTAG automated diffractometer. Samples were analyzed with graphite-monochromatized Cu radiation at 40 kV and 30 mA. The instrument was calibrated using BaF_2 (a = 6.198 Å) and Si (a = 5.430825 Å). Lattice constants were refined using the least-squares program by Appleman and Evans (1973). All three samples were reanalyzed after annealing at 1000 °C.

Petrography

Thorite was found in the quartz zone, quartz–lath spodumene zone, microcline-spodumene zone, and in cleavelandite replacement masses in the beryl zone of the Harding pegmatite in the western end of the main quarry. Detailed descriptions of these units can be found in Jahns and Ewing (1976, 1977) and Lumpkin et al. (1986). The thorium mineral described by Hirschi (1928) was reported to occur in replacement zones in spodumene, presumably within the quartz–lath spodumene zone. The mineral was described as dark brown to ochre-yellow masses or tetragonal prisms associated with albite, muscovite, and quartz (Northrop, 1959).

Most of our samples (HT1, HT2, HT4, HT5) were found in the clevelandite unit where it replaces the beryl zone adjacent to the hanging-wall contact. Thorite occurs as anhedral to euhedral crystals 0.5–8.0 mm in maximum dimension. The color ranges from dark brown to yellow-

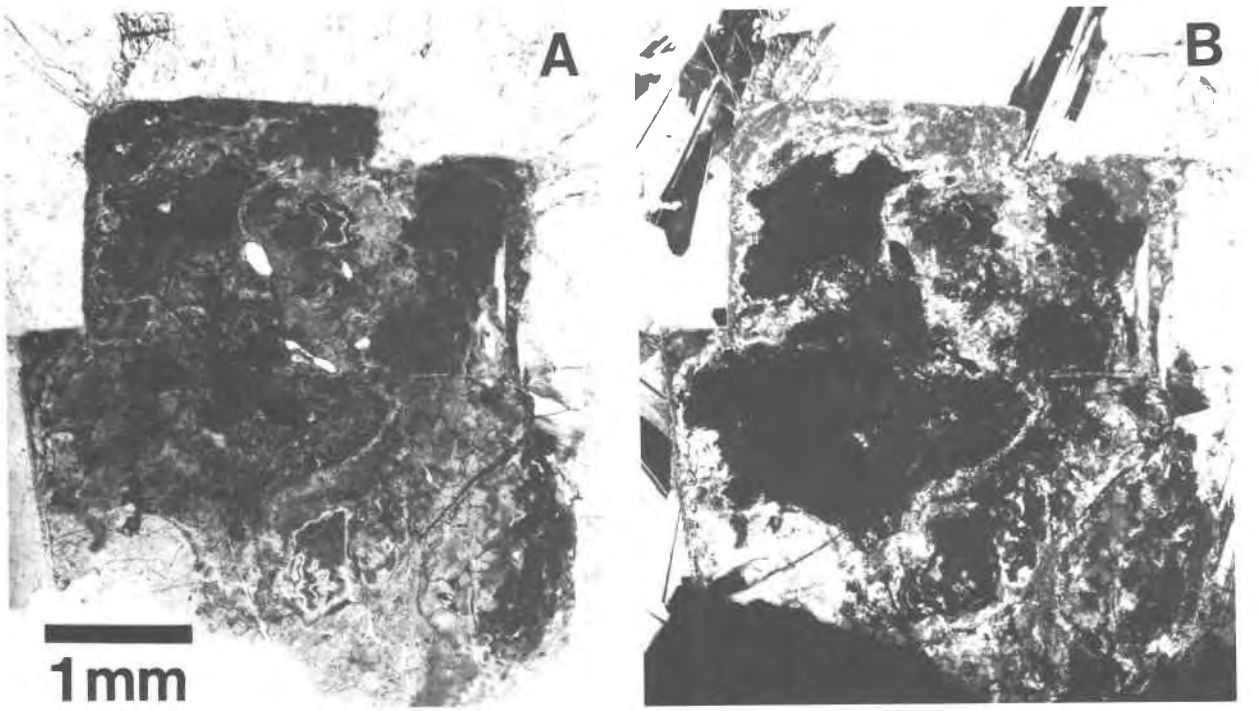

Fig. 1. Photomicrographs of a brown thorite crystal (3 mm) from a cleavelandite mass in the beryl zone. (**A**) View with plane-polarized light shows subhedral outline and mottled texture. (**B**) Viewed with crossed polarizers, some areas within the crystal are isotropic whereas others appear as fine-grained aggregates of anisotropic crystals.

brown. Many crystals have reddish-brown to pale yellow rims. Crystal morphology is simple, consisting of the prism, pinacoid, and pyramid forms. The prism and pinacoid tend to dominate, giving the appearance of "cubic" morphology. Associated minerals are bladed albite, columnar lithian muscovite, quartz, and minor microcline. Mottled blue-green and tan apatite crystals up to 7 cm in length are present in a few specimens.

In thin section (Fig. 1) the thorite grains range from pale yellow to nearly opaque. Inclusions and fracture fillings of orange to red-brown iron oxides are common in many of the crystals. Observation with crossed polarizers reveals that the thorite contains both isotropic and microcrystalline material. Both the ratio of isotropic to crystalline thorite and the size of the crystalline domains are highly variable from grain to grain. The amount of isotropic material is approximately 0–50 vol%. In grains free of isotropic material the crystalline domains approach a maximum size of 200 μm. Crystal rims are occasionally more crystalline than their cores. Sample P20.1, mistaken for microlite by Chakoumakos (1978) is also from a cleavelandite mass in the beryl zone in the westernmost beryl adit. Sample P20.1 exhibits a distinctive texture resembling the recrystallization spherulites observed in metamict polycrase, an orthorhombic Nb-Ta-Ti AB_2O_6 oxide (Ewing, 1974).

A few samples (HT3) occur in the quartz zone as anhedral, tan to yellow masses up to 2 cm in diameter. One sample had a thin brown rim of glassy material surrounding a pale yellow, powdery core. One 2-cm mass in quartz showed a pronounced smoky aureole with radial fractures extending outward into the host quartz. These thorite masses are enclosed within massive quartz, often associated with lithian muscovite.

Other specimens were found in the quartz–lath spodumene zone (HT7) and microcline-spodumene zone (HT6) as <5 mm, chocolate brown to black masses and crystal aggregates associated with zircon. These two samples most closely match those described by Hirschi (1928).

Chemistry

General features

Electron-microprobe analyses of thorites from the cleavelandite unit are given in Tables 1–3. The samples are notable for their high concentrations of P_2O_5, V_2O_5, and CaO. Substantial amounts of Y_2O_3, REE_2O_3, and Bi_2O_3 are also present. Contents of Al_2O_3, Sb_2O_3, MgO, MnO, Na_2O, and Cl are typically below 0.1 wt%. FeO is usually below 0.2 wt%, but higher amounts (up to 15 wt%) occurred where the electron beam impinged upon fine-grained, reddish-colored inclusions. Sample HT2 contained dark red inclusions large enough to analyze. Results most closely resemble the mineral goethite after calculation of Fe as Fe_2O_3. The phase contains small quantities of Al_2O_3 and MgO, but no TiO_2 or MnO. Calculation of enough H_2O to give OH = 1.00 in the structural formula produces an analytical sum near 100 wt%

TABLE 1. Microprobe analyses and formulas of thorite sample HT1 (cleavelandite unit)

	HT1.1		HT1.2		HT1.3		HT1.4		HT1.5	
	Rim	Core	Rim	Core	Rim	Core	Rim	Core	Rim	Core
P_2O_5	7.54	7.56	7.01	5.78	5.66	5.83	7.64	7.68	7.46	7.68
V_2O_5	12.6	13.1	13.3	13.3	13.7	10.1	13.0	12.5	13.2	12.6
As_2O_5	0.30	0.25	0.36	0.59	0.54	0.49	0.33	0.27	0.31	0.25
SiO_2	4.58	4.55	4.88	5.43	5.13	7.62	4.71	4.35	4.73	4.50
ZrO_2	0.58	0.34	0.21	0.18	0.20	0.23	0.26	0.29	0.24	0.22
ThO_2	50.2	50.0	51.4	53.3	53.0	54.7	51.1	50.7	51.5	50.0
UO_2	0.22	0.21	0.17	0.21	0.24	0.32	0.20	0.13	0.21	0.22
Al_2O_3	0.04	0.03	0.04	0.04	0.04	0.32	0.04	0.02	0.03	0.03
Y_2O_3	1.75	1.56	0.96	0.65	0.57	0.33	1.63	1.34	1.80	1.49
REE_2O_3	1.70	1.85	3.43	2.93	3.68	3.31	2.62	2.23	2.81	2.52
Bi_2O_3	2.11	2.16	0.57	0.15	0.13	0.00	1.33	1.63	0.91	1.15
CaO	7.55	7.38	7.62	7.20	7.38	6.29	7.85	7.91	7.44	7.52
FeO	0.01	0.03	0.19	0.06	0.07	0.25	0.09	0.01	0.06	0.00
PbO	0.26	0.30	0.37	0.38	0.33	0.32	0.34	0.21	0.21	0.21
F	0.71	0.72	0.82	0.93	0.96	1.32	0.52	0.75	0.58	0.79
Subtotal	90.18	90.06	91.33	91.13	91.63	91.43	91.68	90.02	91.46	89.20
Less O ≡ F	0.31	0.30	0.34	0.39	0.41	0.55	0.22	0.32	0.24	0.33
Total	89.87	89.76	90.99	90.74	91.22	90.88	91.46	89.70	91.22	88.87
Structural formulas based on O + F = 4.00										
P	0.311	0.310	0.286	0.239	0.233	0.242	0.310	0.318	0.303	0.317
V	0.404	0.419	0.423	0.429	0.440	0.327	0.410	0.404	0.418	0.407
As	0.008	0.007	0.009	0.015	0.014	0.013	0.008	0.007	0.008	0.006
Si	0.223	0.221	0.236	0.265	0.250	0.375	0.225	0.213	0.227	0.220
Al	0.002	0.002	0.002	0.002	0.002	0.018	0.002	0.001	0.002	0.002
ΣB	0.948	0.959	0.956	0.950	0.939	0.975	0.955	0.943	0.958	0.952
Zr	0.015	0.009	0.004	0.004	0.004	0.006	0.006	0.007	0.006	0.006
Th	0.554	0.550	0.562	0.591	0.587	0.608	0.555	0.563	0.561	0.555
U	0.003	0.003	0.001	0.003	0.003	0.003	0.001	0.001	0.003	0.003
Y	0.044	0.040	0.034	0.015	0.016	0.008	0.040	0.033	0.044	0.037
REEs	0.029	0.033	0.059	0.051	0.066	0.059	0.051	0.039	0.048	0.045
Bi	0.025	0.027	0.007	0.002	0.002	0.000	0.017	0.019	0.011	0.013
Ca	0.391	0.381	0.390	0.375	0.386	0.329	0.401	0.413	0.379	0.393
Pb	0.003	0.003	0.006	0.006	0.003	0.003	0.005	0.003	0.003	0.003
ΣA	1.064	1.046	1.063	1.047	1.067	1.016	1.076	1.079	1.055	1.055
F	0.108	0.108	0.124	0.144	0.149	0.203	0.077	0.114	0.089	0.123
O	3.892	3.892	3.876	3.856	3.851	3.797	3.923	3.886	3.911	3.877
H_2O	1.64	1.65	1.43	1.50	1.41	1.47	1.35	1.66	1.39	1.81

and a cation total of 1.003, consistent with the formula of goethite.

The water content of sample HT5 was estimated at ~10 wt% based on TGA analyses giving weight losses of 9.4 and 10.3 wt%. Most of the water was released below 400 °C in steps peaking at 125 and 285 °C for both analyses. Low analytical totals of the microprobe analyses indicate the possible presence of 7.6–11.3 wt% H_2O, consistent with TGA results.

Yellow thorites (Table 3, sample HT3) from the quartz zone have distinctly different compositions in comparison to those from the cleavelandite unit. The samples contain very little P_2O_5 or V_2O_5, and have less Y_2O_3, REE_2O_3, Bi_2O_3, CaO, and F. Major amounts of SiO_2, UO_2, and PbO are characteristic of the yellow thorites. The inferred amounts of H_2O are, on the average, less than those of thorites from the cleavelandite unit. Yellow thorites from the quartz zone of the Harding pegmatite contain the highest PbO contents (up to 17 wt%) yet reported. The maximum UO_2 content approaches 20 wt%. Earlier chemical analyses of thorite samples from other localities indicate a maximum PbO content of 8 wt% and a maximum UO_2 content of 36 wt% (Frondel, 1953, 1958). The high UO_2 content reported by Frondel (1953, 1958) is exceptional; most other chemical analyses indicate a maximum UO_2 content of 20 wt% (Hutton, 1950; Robinson and Abbey, 1957). Recent electron-microprobe data by Foord et al. (1985) give an average of 25 wt% UO_2 in thorite from lithophysal rhyolite, Thomas Mountains, Utah.

Brown thorites from the cleavelandite unit contain the highest concentrations of P_2O_5, V_2O_5, Bi_2O_3, CaO, and F reported to date. Hutton (1950) gave a partial analysis of thorite with 4 wt% P_2O_5. Older analyses of so-called "auerlite" contain 7.4–8.3 wt% P_2O_5 (Hutton, 1950; Frondel, 1958). Most of the analyses reported in the literature have less than 2.0 wt% P_2O_5. This is generally true for CaO as well, exceptions being the U-rich thorites from eastern Ontario that contain 2.1–5.8 wt% CaO (Robinson and Abbey, 1957) and the old analysis of "calciothorite" with 6.9 wt% CaO (Frondel, 1958). V and Bi are not usually determined in routine analyses of thorite. V is a trace constituent in most of the reliable analyses of coffinite, $USiO_4$ (Speer, 1982). Electron-microprobe

Table 2. Microprobe analyses and formulas of thorite samples P20.1 and HT2 (cleavelandite unit)

	P20.1*							HT2.1		HT2.2	
	Rim			Core			Rim	Rim	Core	Rim	Core
P_2O_5	3.86	2.96	5.22	6.25	9.86	10.1	19.5	5.57	5.51	5.57	5.34
V_2O_5	16.2	15.8	14.2	13.1	12.1	10.4	6.41	13.0	10.0	13.7	11.5
As_2O_5	0.83	0.60	0.67	0.77	0.51	0.49	0.27	0.51	0.62	0.52	0.76
SiO_2	4.81	5.14	4.23	4.08	3.38	3.42	2.72	5.29	6.59	5.41	6.87
ZrO_2	0.04	0.07	0.02	0.07	0.14	0.09	0.02	0.13	0.20	0.11	0.10
ThO_2	53.1	52.8	51.0	50.4	51.0	49.1	42.9	53.3	55.8	53.0	55.2
UO_2	0.62	0.88	0.57	0.69	0.21	0.20	0.05	0.32	0.26	0.17	0.31
Al_2O_3	0.09	0.07	0.07	0.06	0.06	0.11	0.08	0.05	0.05	0.06	0.05
Y_2O_3	1.89	1.74	1.79	2.36	2.89	2.59	2.63	1.02	0.76	0.79	0.52
REE_2O_3	2.62	2.76	2.65	3.02	2.70	2.73	6.45	3.05	3.01	3.27	3.28
Bi_2O_3	0.00	0.09	0.04	0.12	0.00	0.00	0.00	0.00	0.00	0.02	0.01
CaO	6.74	6.86	7.12	7.34	7.48	8.24	8.26	6.49	5.84	7.27	6.66
FeO	0.36	0.11	0.09	0.09	0.02	0.17	0.13	0.11	0.04	0.37	0.24
PbO	0.34	0.34	0.27	0.17	0.14	0.27	0.19	0.47	0.22	0.28	0.24
F	1.08	1.09	1.45	1.60	1.07	1.30	1.14	0.97	1.15	1.19	1.13
Subtotal	92.68	91.32	89.40	90.14	91.58	89.22	90.82	91.38	91.78	91.84	92.20
Less O ≡ F	0.45	0.46	0.61	0.67	0.45	0.55	0.48	0.41	0.48	0.50	0.47
Total	92.23	90.86	88.79	89.47	91.13	88.67	90.34	90.97	91.30	91.34	91.73
Structural formulas based on O + F = 4.00											
P	0.159	0.127	0.220	0.262	0.393	0.412	0.692	0.235	0.245	0.230	0.223
V	0.522	0.522	0.467	0.427	0.376	0.331	0.177	0.428	0.334	0.440	0.372
As	0.021	0.016	0.018	0.020	0.012	0.013	0.006	0.013	0.017	0.013	0.020
Si	0.233	0.257	0.211	0.203	0.160	0.165	0.115	0.263	0.333	0.263	0.338
Al	0.006	0.003	0.004	0.003	0.004	0.006	0.003	0.004	0.004	0.004	0.004
ΣB	0.941	0.925	0.920	0.915	0.945	0.927	0.993	0.943	0.933	0.950	0.957
Zr	0.001	0.001	0.000	0.001	0.003	0.001	0.000	0.003	0.004	0.003	0.003
Th	0.586	0.599	0.578	0.560	0.543	0.538	0.409	0.601	0.638	0.583	0.613
U	0.007	0.010	0.006	0.007	0.003	0.001	0.000	0.003	0.003	0.001	0.003
Y	0.049	0.045	0.048	0.059	0.071	0.065	0.059	0.025	0.020	0.019	0.014
REEs	0.047	0.050	0.048	0.053	0.045	0.048	0.099	0.055	0.054	0.058	0.058
Bi	0.000	0.000	0.000	0.002	0.000	0.000	0.000	0.014	0.018	0.002	0.000
Ca	0.350	0.365	0.380	0.383	0.374	0.425	0.370	0.343	0.314	0.376	0.346
Pb	0.006	0.003	0.003	0.002	0.002	0.003	0.003	0.006	0.003	0.003	0.003
ΣA	1.046	1.073	1.063	1.067	1.041	1.081	0.940	1.050	1.054	1.045	1.040
F	0.166	0.183	0.228	0.248	0.158	0.197	0.151	0.149	0.182	0.181	0.176
O	3.834	3.817	3.772	3.752	3.842	3.803	3.849	3.851	3.818	3.819	3.824
H_2O	1.25	1.50	1.85	1.70	1.38	1.80	1.34	1.49	1.44	1.40	1.33

* Analyses range from rim to core (center column) to rim in the order given.

analysis of coffinite from the Woodrow mine, Grants County, New Mexico revealed 0.64 wt% V_2O_5 along with 2.18 wt% P_2O_5 and 2.34 wt% CaO (Kim, 1978). Speer (1982) listed F and Cl as questionable minor constituents. Our electron-microprobe analyses provide conclusive evidence for the presence of F in amounts approaching 1.6 wt% (Tables 1–3).

Microprobe analyses of thorites from the quartz–lath spodumene zone (HT7) and microcline-spodumene zone (HT6) are listed in Table 4. Sample HT7 most closely approaches ideal thorite in composition, containing moderate amounts of UO_2 (4.0–8.6 wt%) and PbO (2.5–4.8 wt%), and negligible water. Only occasional spots showed as much as 0.4 wt% Al_2O_3, 1.8 wt% CaO, and 0.4 wt% F, possibly owing to incipient alteration. In contrast, sample HT6 from the microcline-spodumene zone contains relatively unaltered areas close to end member $ThSiO_4$ in composition and moderately altered areas enriched in P, V, As, and Ca (Table 4). Analytical totals indicate H_2O contents of 0–10% wt%, clustering near 4–5 wt% for altered areas. Alteration of sample HT6 appears to be related to partial albitization of the microcline-spodumene zone.

Stoichiometry

Structural formulas of the Harding thorites were calculated on the basis of 4.00 O + F anions. Water contents are estimated by difference and calculated as H_2O. Values of ΣA and ΣB allow for further interpretation of the role of water in the structure.

A-site cations. Thorites from the cleavelandite unit contain 0.40–0.65 Th, 0.28–0.43 Ca, 0.00–0.10 REEs, 0.00–0.08 Y, and 0.00–0.06 Bi atoms per formula unit. Concentrations of Zr, U, and Pb are below 0.01 atoms per formula unit. In contrast, yellow thorites from the quartz zone contain 0.46–0.79 Th, 0.05–0.22 U, 0.05–0.22 Pb, and 0.05–0.08 Ca atoms per formula unit (see Tables 1–3). The relative variation of A-site cations grouped according to valence is depicted in Figure 2. Samples from the cleavelandite unit contain the greatest amounts of divalent and trivalent cations, approaching 45 mol% A^{2+} and 20 mol% A^{3+} cations in sample P20.1.

TABLE 3. Microprobe analyses and formulas of thorite samples HT3, HT4, and HT5

	HT3				HT4			HT5		
P_2O_5	0.15	0.18	0.19	0.14	5.17	5.01	5.45	7.44	6.42	5.11
V_2O_5	0.09	0.08	0.04	0.10	14.4	12.4	10.8	10.8	10.4	10.2
As_2O_5	0.24	0.26	0.28	0.24	0.61	0.86	1.18	0.26	0.55	0.46
SiO_2	17.5	18.5	18.0	17.8	4.96	5.77	6.34	5.43	6.56	7.26
ZrO_2	0.52	0.55	0.60	0.42	0.23	0.25	0.27	0.16	0.12	0.10
ThO_2	62.8	61.4	56.5	37.6	53.9	55.2	54.9	52.7	52.6	55.7
UO_2	4.55	4.75	7.65	18.8	0.19	0.18	0.24	0.19	0.29	0.27
Al_2O_3	0.76	0.69	0.73	0.47	0.12	0.06	0.11	0.05	0.08	0.00
Y_2O_3	0.33	0.54	0.56	0.51	0.14	0.10	0.12	1.23	1.27	0.81
REE_2O_3	0.26	0.21	0.21	0.54	0.10	0.49	0.14	2.88	3.53	3.19
Bi_2O_3	0.64	0.94	0.72	0.79	4.07	4.54	4.58	2.77	3.18	0.62
CaO	1.24	0.99	0.90	0.82	7.27	6.70	6.31	6.54	5.97	5.28
FeO	0.04	0.33	0.19	0.18	0.00	0.00	0.12	0.10	0.06	0.00
PbO	3.84	4.63	7.65	16.4	0.57	0.28	0.25	0.46	0.24	0.35
F	0.61	0.89	0.80	0.05	0.96	0.72	0.95	0.78	1.47	0.94
Subtotal	93.57	94.95	95.02	94.87	92.69	92.56	91.76	91.79	92.74	90.30
Less O ≡ F	0.26	0.37	0.34	0.02	0.40	0.30	0.40	0.33	0.62	0.39
Total	93.31	94.58	94.68	94.85	91.29	92.26	91.36	91.46	92.12	89.91
Structural formulas based on O + F = 4.00										
P	0.006	0.007	0.008	0.007	0.214	0.216	0.233	0.311	0.266	0.221
V	0.002	0.002	0.001	0.003	0.466	0.418	0.360	0.353	0.337	0.345
As	0.006	0.007	0.008	0.007	0.015	0.023	0.032	0.007	0.014	0.012
Si	0.959	0.983	0.967	0.976	0.243	0.295	0.320	0.269	0.322	0.372
Al	0.048	0.042	0.046	0.029	0.008	0.004	0.008	0.002	0.004	0.000
ΣB	1.021	1.041	1.030	1.022	0.946	0.956	0.953	0.942	0.943	0.950
Zr	0.015	0.014	0.016	0.012	0.006	0.006	0.006	0.004	0.003	0.003
Th	0.784	0.743	0.692	0.470	0.600	0.641	0.628	0.591	0.583	0.647
U	0.053	0.054	0.086	0.215	0.001	0.001	0.003	0.001	0.003	0.003
Y	0.009	0.015	0.018	0.015	0.004	0.002	0.002	0.031	0.031	0.021
REEs	0.004	0.004	0.004	0.011	0.002	0.007	0.002	0.051	0.062	0.059
Bi	0.009	0.013	0.011	0.011	0.051	0.059	0.058	0.033	0.039	0.008
Ca	0.072	0.058	0.052	0.050	0.379	0.365	0.338	0.344	0.311	0.289
Pb	0.056	0.067	0.113	0.214	0.006	0.003	0.003	0.006	0.003	0.006
ΣA	1.002	0.968	0.992	0.988	1.049	1.084	1.040	1.061	1.035	1.036
F	0.105	0.150	0.137	0.010	0.150	0.117	0.152	0.122	0.226	0.151
O	3.895	3.850	3.863	3.990	3.850	3.883	3.848	3.878	3.774	3.849
H_2O	1.20	1.08	0.93	0.88	1.24	1.30	1.45	1.38	1.27	1.71

Note: Sample HT3 is from the quartz zone; HT4 an HT5 are from the cleavelandite unit.

Sample HT3 from the quartz zone contains only 15–30 mol% A^{2+} and 1–3 mol% A^{3+} cations. Individual A^{3+} cations are plotted in Figure 3. Sample HT3 has Y as the dominant A^{3+} cation, but contains significant amounts of REEs and Bi. Among samples from the cleavelandite unit, HT4 is Bi rich, whereas most other samples are enriched in the REEs.

Relative abundances of the REEs (normalized to Ce = 1.0) are summarized in Figure 4. The light REEs are dominant in all specimens, of which five showed Ce-dominant patterns and three showed La-dominant patterns. La/Ce ratios range widely from 0.4 to 1.4. Low REE contents of samples HT3, HT4, HT6, and HT7 precluded determination of complete REE distributions; however, Ce was the major REE found in all four specimens. Prior to this work, Staatz et al. (1976) analyzed four thorites from the Seerie pegmatite, Jefferson County, Colorado, and found all four to be Yb dominant. Staatz et al. (1976) also made a literature survey of thorite analyses, finding five Ce-dominant, two Nd-dominant, and two Dy-dominant.

Sample HT7 from the quartz–lath spodumene zone closely approaches ABO_4 stoichiometry. The average composition of the A site is 0.87 Th, 0.08 U, and 0.05 Pb atoms per formula unit. Maximum values of 0.10 Ca and 0.02 Mn atoms per formula unit occur in small areas of the specimen and may be related to incipient alteration. Partial alteration of sample HT6 from the microcline-spodumene zone produced a wide range in the number of A-site cations: 0.73–0.87 Th, 0.01–0.04 U, and 0.10–0.26 Ca atoms per formula unit. The amounts of Y, REEs, Mn, and Pb are generally below 0.01 atoms per formula unit (Table 4).

B-site cations. Brown thorites from the cleavelandite unit have complex B-site compositions involving 0.12–0.70 P, 0.17–0.53 V, 0.11–0.38 Si, and 0.01–0.04 As atoms per formula unit. Al contents are generally below 0.01 atoms per formula unit. Yellow thorite HT3 has a relatively simple B-site composition of 0.95–0.99 Si and 0.02–0.06 Al atoms per formula unit. Amounts of P, V, and As are below 0.01 atoms per formula unit (Tables 1–3). Except for small amounts of Al (<0.03 atoms per formula unit), the B site of sample HT7 is fully occupied by Si. On the other hand, sample HT6 contains 0.01–

TABLE 4. Microprobe analyses and formulas of thorite samples HT6 and HT7

	HT6						HT7			
P_2O_5	0.31	0.38	2.03	2.29	4.24	7.00	0.00	0.00	0.00	0.00
V_2O_5	0.28	0.12	0.14	4.60	4.12	6.00	0.07	0.04	0.04	0.02
As_2O_5	0.21	0.19	0.15	1.80	0.75	0.55	0.04	0.02	0.03	0.03
SiO_2	19.0	19.3	17.7	11.8	11.5	7.81	18.3	18.7	18.6	18.6
ZrO_2	0.32	0.48	1.03	2.60	0.54	1.57	0.03	0.02	0.00	0.00
ThO_2	74.6	69.4	67.4	61.2	67.8	65.7	69.5	70.1	70.2	69.3
UO_2	1.75	2.21	3.41	0.76	1.84	1.67	6.67	6.71	5.60	6.18
Al_2O_3	0.27	0.62	0.47	0.17	0.87	0.23	0.06	0.05	0.06	0.36
Y_2O_3	0.00	0.00	0.00	0.00	0.00	0.04	0.07	0.09	0.10	0.00
REE_2O_3	0.33	0.11	0.19	0.01	0.18	0.25	0.37	0.41	0.55	0.11
Bi_2O_3	0.00	0.00	0.00	0.00	0.00	0.02	—	—	—	—
CaO	2.06	2.65	1.93	4.42	2.77	3.81	0.06	0.01	0.02	1.70
FeO	0.07	0.06	0.04	0.02	0.06	0.03	0.00	0.02	0.01	0.00
PbO	0.46	0.28	0.21	0.07	0.21	0.19	3.61	3.99	4.01	1.34
F	0.76	0.3	0.85	0.75	0.83	0.60	0.19	0.06	0.10	0.33
Subtotal	100.42	96.03	95.55	90.49	95.71	95.37	98.97	100.22	99.32	97.97
Less O ≡ F	0.32	0.10	0.36	0.32	0.35	0.21	0.08	0.03	0.04	0.14
Total	100.10	95.93	95.19	90.17	95.36	95.16	98.89	100.19	99.28	97.83
Structural formulas based on O + F = 4.00										
P	0.013	0.017	0.088	0.103	0.184	0.300	0.000	0.000	0.000	0.000
V	0.009	0.004	0.005	0.161	0.140	0.201	0.002	0.001	0.001	0.001
As	0.006	0.005	0.004	0.050	0.020	0.015	0.001	0.000	0.001	0.001
Si	0.964	0.995	0.909	0.626	0.590	0.396	1.003	1.008	1.014	0.992
Al	0.016	0.038	0.028	0.011	0.053	0.014	0.004	0.003	0.004	0.022
ΣB	1.008	1.059	1.034	0.951	0.987	0.926	1.010	1.012	1.020	1.016
Zr	0.008	0.012	0.026	0.067	0.014	0.039	0.001	0.001	0.000	0.000
Th	0.862	0.815	0.788	0.739	0.792	0.758	0.866	0.861	0.868	0.842
U	0.020	0.025	0.039	0.009	0.021	0.019	0.081	0.081	0.067	0.073
Y	0.000	0.000	0.000	0.000	0.000	0.001	0.002	0.003	0.003	0.000
REE	0.006	0.002	0.003	0.000	0.003	0.005	0.007	0.008	0.010	0.002
Bi	0.000	0.000	0.000	0.000	0.000	0.000	—	—	—	—
Ca	0.112	0.146	0.106	0.251	0.152	0.207	0.003	0.000	0.001	0.097
Pb	0.006	0.004	0.003	0.001	0.003	0.003	0.053	0.057	0.058	0.019
ΣA	1.014	1.004	0.965	1.067	0.985	1.032	1.013	1.011	1.007	1.033
F	0.121	0.042	0.139	0.131	0.137	0.100	0.033	0.010	0.017	0.057
O	3.879	3.958	3.861	3.869	3.863	3.900	3.967	3.990	3.983	3.943
H_2O	—	0.65	0.77	1.73	0.77	0.79	—	—	—	—

Note: Sample HT6 is from the microcline-spodumene zone, HT7 is from the quartz-lath spodumene zone.

0.31 P, 0.00–0.21 V, 0.00–0.05 As, 0.39–1.00 Si, and 0.01–0.05 Al atoms per formula unit, reflecting the partially altered nature of the specimen (Table 4).

Relative amounts of Si, P, and V are plotted in Figure 5. Except for samples HT3, HT7, and unaltered areas of HT6, the B-site compositions of the Harding thorites are unique. Most data points of samples from the cleavelandite unit have V as the major B-site cation (up to 60 mol%). A few analyses have Si as the dominant B-site cation (up to 50 mol%). The most interesting results were found for sample P20.1. Data points for P20.1 scatter along a line of constant V/Si = 2.0 over a range of 10–70 mol% P. Most data points, however, cluster just inside the P-dominant composition field near 42 mol% P, 40 mol% V, and 18 mol% Si. Alteration of sample HT6 from the microcline-spodumene zone is revealed by the trend of data points that lie within the Si-dominant field along a line of constant P/V = 1.0 (Fig. 5).

A literature survey of thorite and xenotime analyses indicates maximum substitution of 20 mol% Si in xenotime and 15 mol% P in thorite (Palache et al., 1944; Robinson and Abbey, 1957; Frondel, 1958; Heinrich, 1963; Åmli, 1975; Staatz et al., 1976). V was not determined in these analyses, but is probably very low in abundance. Based on X-ray fluorescence analyses that showed 11 wt% Y and 3 wt% V in thorite ("thorogummite") from the Evans-Lou pegmatite, Quebec, Miles et al. (1971) suggested the substitution of ~10 mol% V for Si. They also inferred the possible substitution of ~10 mol% P for Si, presumably to balance excess amounts of Y. Miles et al. (1971) also described wakefieldite from the Evans-Lou pegmatite, but did not obtain a good analysis of the mineral because of impurities. In addition to SiO_2, several weight percent of ThO_2 and UO_2 may in fact be present in wakefieldite (Miles et al., 1971, p. 401 and their Table 5). Using the unit-cell volumes of natural wakefieldite, synthetic YVO_4, $ThSiO_4$, and $USiO_4$, we estimate a maximum possible substitution of ~20 mol% Si for V in wakefieldite.

Anions and water. F contents of samples from the cleavelandite unit range from 0.07 to 0.25 atoms per formula unit. Sample HT3 from the quartz zone contains 0.01–0.16 F atoms per formula unit. Partially altered thorite HT6 from the microcline-spodumene zone contains 0.03–0.15 F atoms per formula unit. Relatively unaltered material (HT7) from the quartz–lath spodumene

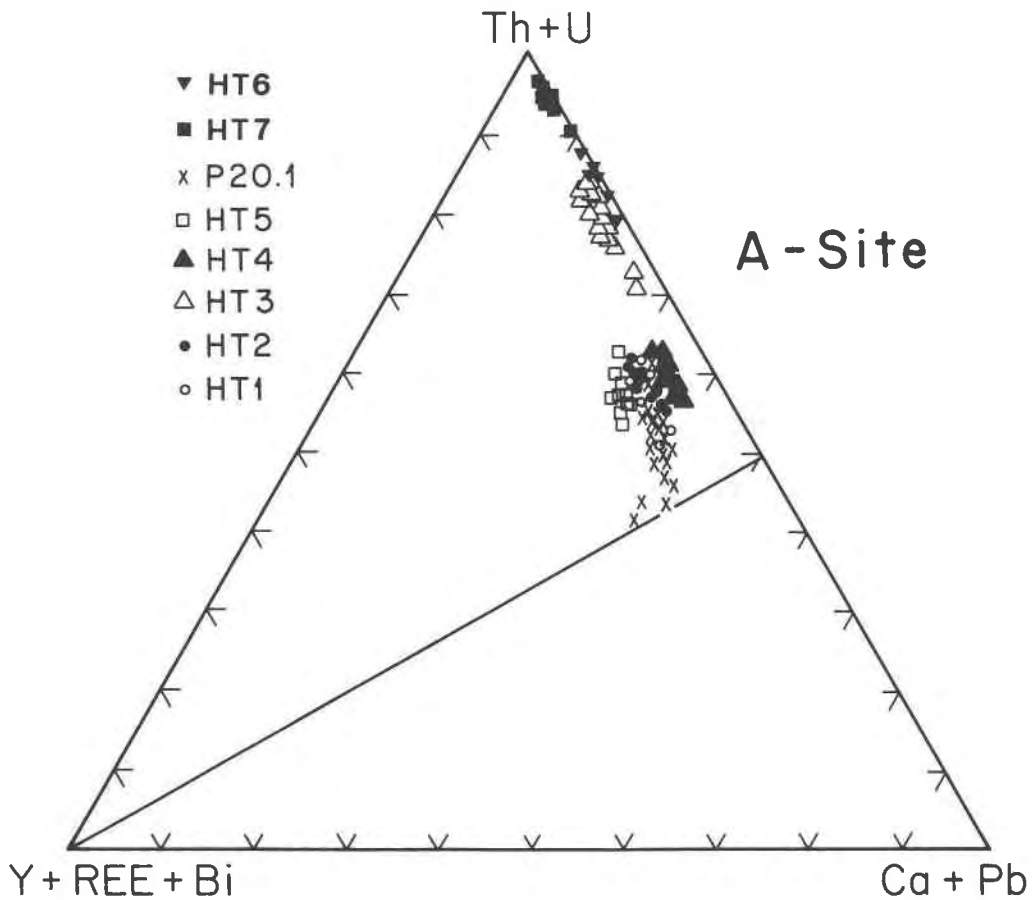

Fig. 2. Ternary plot of A-site cations grouped according to valence state. Samples from the cleavelandite unit cluster near 35 mol% A^{2+} and 10 mol% A^{3+} cations, approaching 45 mol% A^{2+} and 20 mol% A^{3+} cations in sample P20.1. Samples from primary lithologic units are dominated by A^{4+} cations.

zone contains only 0.00–0.06 F atoms per formula unit. Oxygen contents of all samples range from 3.75 to 4.00 atoms per formula unit. Water contents of the samples were estimated by difference and calculated as H_2O. Samples from the cleavelandite unit contain 1.2–1.9 H_2O molecules per formula unit. Lower water contents of 0.8–1.6 H_2O molecules per formula unit are inferred for sample HT3. Sample HT6 has an inferred water content of 0.0–1.8 H_2O molecules per formula unit, with higher water contents associated with altered areas of the specimen. However, most analyses of altered material contain 0.6–0.8 H_2O molecules per formula unit.

The role of water in the structure can be inferred from the H_2O content and values of ΣA and ΣB by plotting on a ternary diagram (Mumpton and Roy, 1961). Figure 6 shows that data for thorites HT3 and HT6 scatter along the ABO_4-H_2O join. Data for samples from the cleavelandite unit scatter just below the ABO_4-H_2O join, indicating that there are B-site vacancies and possible OH groups due to the substitution of $4H^+$ for Si^{4+}. The magnitude of this substitution must be small, because mean values of ΣA and ΣB are 1.05 and 0.95, respectively. Although marginal, this departure from perfect stoichiometry appears to be real. Based on counting statistics, the 1σ standard deviations on ΣA and ΣB are both near ±0.01 atoms per formula unit. Normalizing to ΣA = 1.00, we get ΣB = 0.90 and 0.10 B-site vacancies by difference. The maximum amount of H^+ required to fill all B-site vacancies is 0.4 ± 0.1 atoms per formula unit. The large standard deviation arises from uncertainties in estimating the total H_2O content by difference. As discussed below, infrared spectroscopy confirms the presence of molecular water and is consistent with the presence of hydroxyl species.

Infrared spectroscopy

The IR spectrum (Fig. 7) of yellow thorite HT3 shows an absorption at 1630 cm^{-1} that is identified as the H–O–H bending mode of molecular water. The O–H stretching modes of molecular water and hydroxyl species are indicated by the band at 3400 cm^{-1}, whose large breadth is evidence of molecular water and hydroxyl species that are not in a single well-defined site or of a consistent type (Aines and Rossman, 1986).

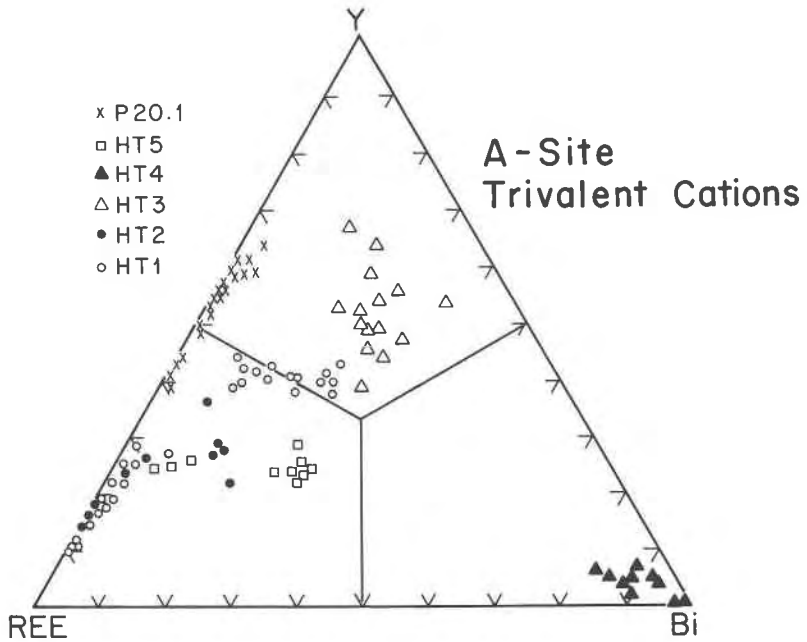

Fig. 3. Ternary plot of the trivalent cations Y, REEs, and Bi (mol%). Note the gap between Bi-poor and Bi-rich compositions.

The IR spectrum of brown thorite HT5 (Fig. 7) is similar to that of sample HT3, but with additional absorption bands at 1540 and 1350 cm^{-1}. The broad band at 3200 cm^{-1} appears to be a composite of the 3400 cm^{-1} band due to O–H stretching in H_2O and OH, plus an additional broad band at lower wave numbers from $(PO_4)^{3-}$. The double band at 1540 and 1350 cm^{-1} is characteristic of the carbonate anion, $(CO_3)^{2-}$, suggesting the presence of an additional carbonate phase as an alteration product of thorite. However, no carbonate phases have been identified by optical microscopy, X-ray diffraction analysis, or transmission electron microscopy.

Intracrystalline zoning

Core-to-rim variations in composition of most thorite grains are minor. When pronounced zoning is observed, cores are richer in Si and Th, and rims tend to be enriched in V, P, and Ca (i.e., sample HT1, Table 1). In general, absolute concentrations of Y, REEs, and Bi are also higher in crystal rims. On a relative basis, the core-to-rim trend of A^{3+} cations proceeds from REEs to Y to Bi along curved paths (Fig. 3).

The most spectacular zoning was observed in sample P20.1. The zoning pattern is not concentric; compositional variations occur between two opposite sides of the grain. One side of the grain is rich in V, Si, and Th and has higher amounts of the minor elements As and U. The opposite side is rich in P with increased amounts of Y, REEs, and Ca. B-site cations follow the V/Si = 2.00 trend shown in Figure 5. F and B-site vacancies reach maximum values near the middle of the grain and have minimum values near the V-rich and P-rich edges.

Compositional variations were observed in several grains removed from sample HT3. Figure 8 shows that U and Pb scatter near the 1:1 correlation line. Linear-regression analysis of the data yielded a slope of 0.952 and a correlation coefficient of 0.973. Unfortunately, the powdery nature of the specimen has made it difficult to prepare an adequate polished section. As a result, we have not analyzed enough of the sample to establish any spatial zoning pattern.

Substitution schemes

The major substitutions indicated by core-to-rim zoning in samples HT1, HT2, HT4, and HT5 are $^{A}Ca^{B}V_2 \rightarrow {}^{A}Th^{B}Si_2$ and $^{A}Ca^{B}P_2 \rightarrow {}^{A}Th^{B}Si_2$ (Tables 1–4, Figs. 2–6). In sample HT4 the substitution is predominantly of the first type as indicated by the trend of data points in Figure

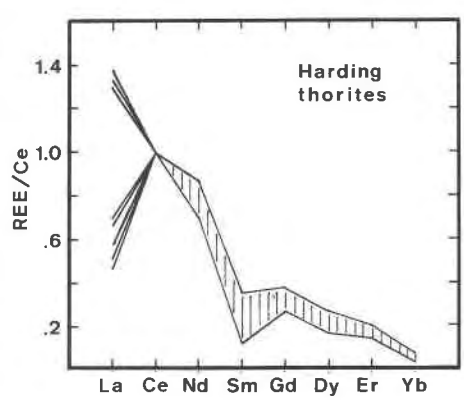

Fig. 4. REE distributions (atom ratios) of Harding thorites normalized to Ce = 1.00. Individual data points are shown only for La/Ce. Minimum and maximum REE/Ce values are plotted for Nd–Yb.

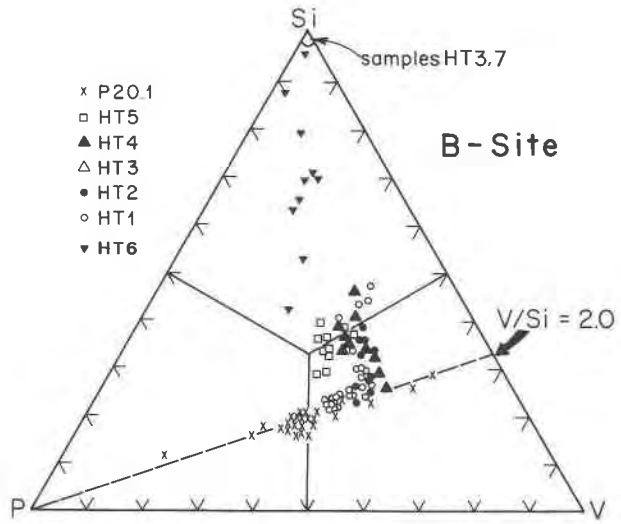

Fig. 5. Ternary plot of B-site cations Si, P, and V (mol%). Data for sample P20.1 scatter along a line of constant V/Si = 2.0 from 10 to 70 mol%, clustering near 42 mol% P. Most other data points for samples from the cleavelandite unit lie within the V-dominant composition field, extending just into the Si-dominant field. Samples from primary lithologic units contain Si as the major B-site cation.

5. In samples HT1, HT2, and HT5 the two substitutions operate in roughly equal proportions. This is also true of the alteration pattern in specimen HT6. A general substitution scheme for these four samples is $^{A}Ca^{B}V^{B}P \rightarrow {}^{A}Th^{B}Si_2$. The unusual zoning pattern in sample P20.1 is consistent with the major substitutions $^{B}P \rightarrow {}^{B}V$ and

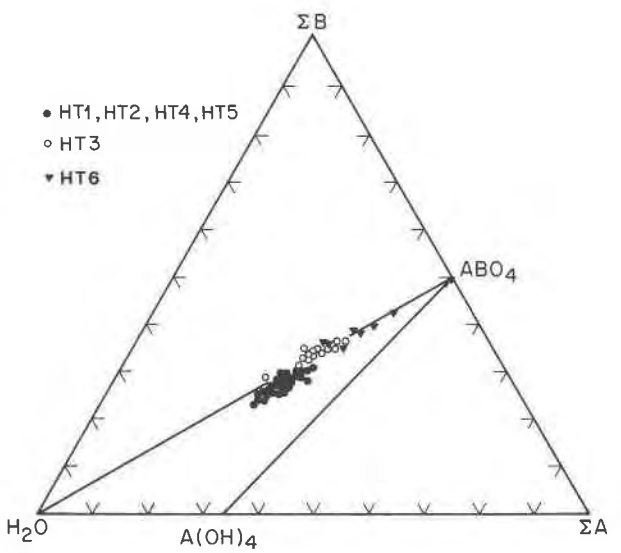

Fig. 6. Ternary diagram of ΣA, ΣB, and H_2O (mol%). Data for samples from primary lithologic units scatter along the ABO_4-H_2O join. Samples from the cleavelandite replacement unit scatter just below the ABO_4-H_2O join, consistent with a small amount of H^+ at the B site.

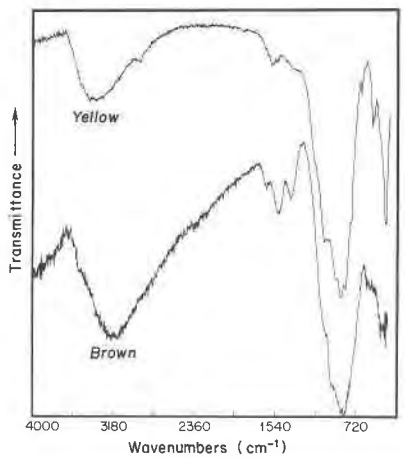

Fig. 7. FT-IR patterns for yellow thorite HT3 and brown thorite HT5.

$^{A}REE^{B}P \rightarrow {}^{A}Th^{B}Si$. As shown in Figure 5, P increases along a line of constant V/Si = 2.0, such that a generalized substitution scheme can be written as $^{A}REE^{B}P_3 \rightarrow {}^{A}Th^{B}Si^{B}V_2$. Obviously, minor substitutions like $^{A}Y^{B}P \rightarrow {}^{A}Th^{B}Si$, $^{A}Y^{B}V \rightarrow {}^{A}Th^{B}Si$, and $^{A}Bi^{B}V \rightarrow {}^{A}Th^{B}Si$ also play a role in the crystal chemistry of these samples.

Approximate 1:1 variation of U and Pb in sample HT3 provides evidence for the substitution $^{A}Pb^{A}U^{6+} \rightarrow {}^{A}Th_2$ (Fig. 8). Most of the U in this sample is probably present as the U^{6+} ion. A possible minor substitution accounting for the occurrence of Al and F in HT3 can be expressed as $^{B}Al^{X}F \rightarrow {}^{B}Si^{X}O$. In general, the substitution of F for O serves to charge-balance excess low-valence cations in the structure, preventing instability due to underbonding at the anion site.

Figure 9 presents a summary of Harding thorite compositions expressed in terms of idealized end members. Samples from the cleavelandite unit contain 50–75 mol%

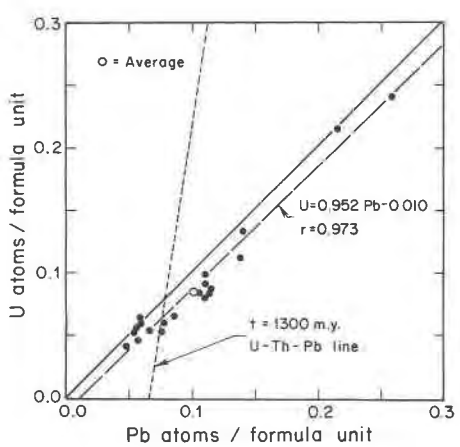

Fig. 8. A plot of U vs. Pb (mol%) for sample HT3. Data points scatter near the 1:1 U:Pb line, well off the calculated 1300-m.y. U-Th-Pb line. The average composition (open circle) does plot near the 1300-m.y. reference line.

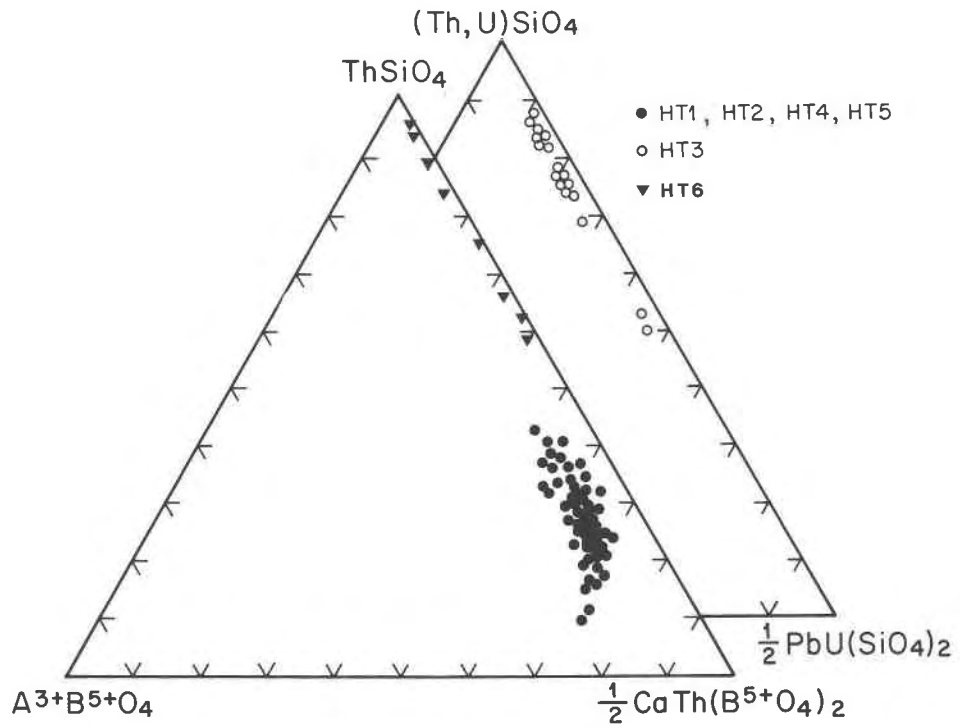

Fig. 9. Harding thorite compositions plotted in terms of idealized end members (mol%). Samples from the cleavelandite unit are dominated by the component $CaTh(B^{5+}O_4)_2$, where B = P and V. A sample (HT3) from the quartz zone is near–end member $(Th,U)SiO_4$, but exhibits extensive substitution toward $PbU(SiO_4)_2$.

of the $CaTh(B^{5+}O_4)_2$ component and 5–20 mol% of the $A^{3+}B^{5+}O_4$ component. Specimen HT3 typically contains 10–30 mol% $PbU(SiO_4)_2$ in substitution for $ThSiO_4$. Two analyses of sample HT3 approach a maximum of 50 mol% of the $PbU(SiO_4)_2$ end member (Fig. 9).

Structure and radiation effects

The dose (α/mg) and number of displacements per atom (dpa) have been calculated for all of the thorite samples. It is common to calculate dose in units of α/m^3, but this approach requires a measured value of density, which decreases with increasing dose. Therefore, we calculated the dose in units of α/mg following a modified procedure from Holland and Gottfried (1955) based on the decay schemes of ^{232}Th and ^{238}U. No consideration was given to alpha decay of ^{235}U. An age of 1300 m.y. was used (Brookins et al., 1979). With each alpha decay, a recoil nucleus (0.1 MeV) and an alpha particle (5.5 MeV) are produced. The range of the alpha particle is approximately 10 μm, but its energy is dissipated mainly by ionization events along its trajectory, producing 100–200 atomic displacements near the end of its path. The recoil nucleus has a maximum range of 0.1 μm, but because of its greater mass, it produces 1000–2000 atomic displacements. Values of dpa were calculated assuming 1500 atomic displacements per alpha-decay event. Calculated doses are in the range of 5–12 $\times$ 10^{17} α/mg for samples HT3, HT6, and HT7 and 4–5 $\times$ 10^{17} α/mg for samples HT1, HT2, HT4, and HT5. Corresponding dpa values are in the range of 25–40 for all samples.

X-ray diffraction patterns of unannealed thorite samples exhibit two broad humps at 3.0 and 1.8 Å that are characteristic of an aperiodic (metamict) structure, with weak Bragg reflections superimposed. This type of pattern indicates a mixture of crystalline and metamict thorite, consistent with petrographic observations. After annealing at 1000 °C in air, the intensity of the Bragg reflections increase by a factor of 3–4, and the two broad humps disappear. Both unheated and annealed patterns can be indexed based on a thorite unit cell. Refined lattice constants of samples HT3, HT4, and HT5 are given in Table 5 along with data for synthetic compounds having the zircon structure type.

Transmission electron microscopy of sample HT5 reveals coexisting regions of aperiodic (metamict) and crystalline material (Fig. 10). The upper left side of the HRTEM image is predominantly aperiodic. Lattice fringes occur infrequently and rare, 10- to 20-Å crystallites can be observed only with careful scrutiny. The electron-diffraction pattern from this part of the image shows diffuse diffraction halos with equivalent d spacings of 3.1 and 1.9 Å, close to values estimated by X-ray diffraction anlaysis. A few weak diffraction rings and spots are also visible. The right side of the HRTEM image contains both crystalline and aperiodic domains in the 50- to 500-Å size range. Lattice fringes appear to be randomly oriented. The elec-

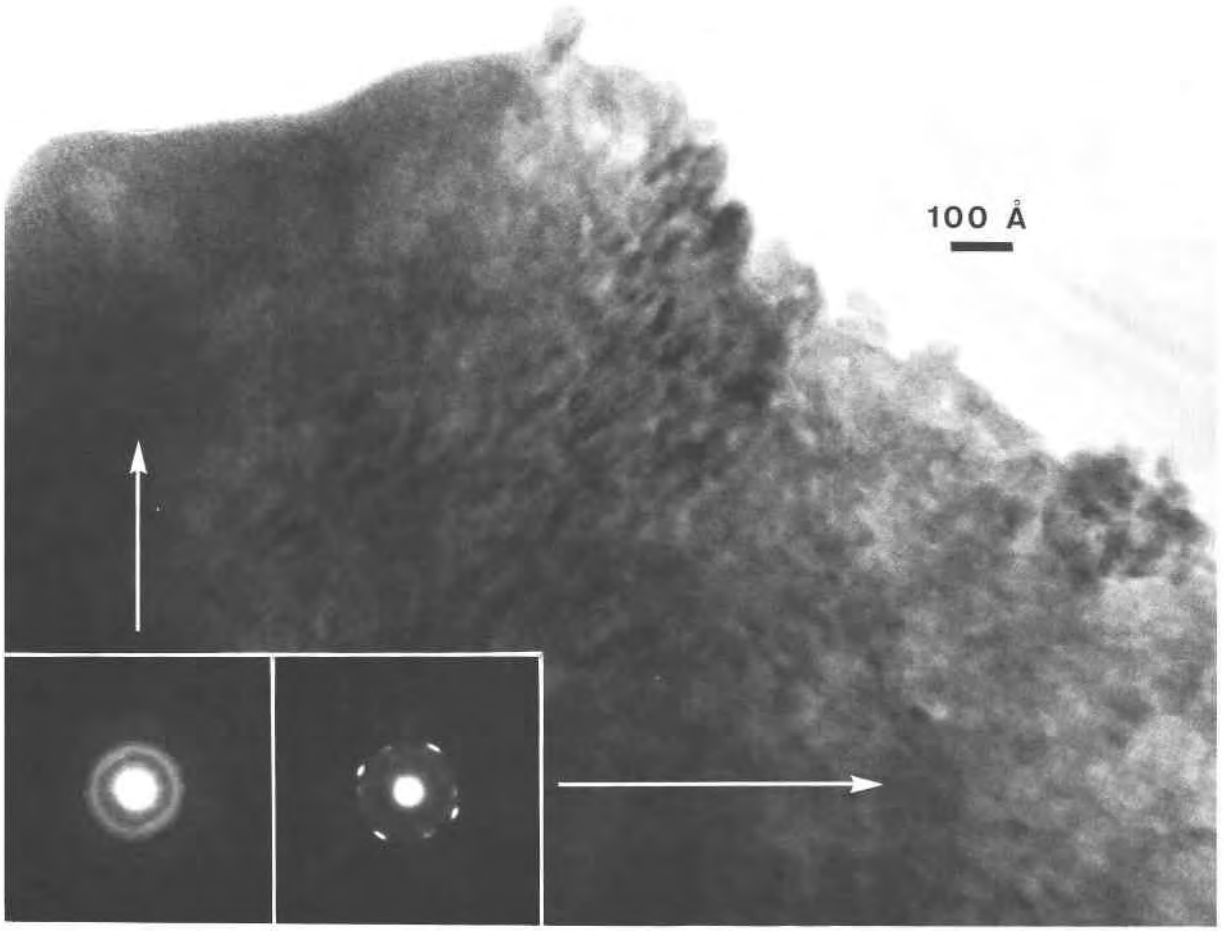

Fig. 10. HRTEM image and electron-diffraction patterns of brown thorite HT5 from the cleavelandite unit. Arrows indicate regions where diffraction patterns were taken.

tron-diffraction pattern from this part of the image exhibits diffraction spots and weaker diffuse halos. Diffraction spots are actually streaked into short arcs, indicating lattice distortion of 10–15°. Crystalline domains have *d* spacings consistent with the zircon structure type.

Discussion

Paragenesis

The occurrence of rather large subhedral crystals of thorite in the quartz zone is consistent with relatively early formation during crystallization of the pegmatite. Microprobe analyses indicate that the primary composition of thorite was close to ideal $ThSiO_4$, but enriched in U. Additional primary thorite containing lesser amounts of U crystallized in the quartz–lath spodumene zone and the microcline-spodumene zone in association with hafnian zircon. Brown thorites crystallized later during subsolidus replacement of the beryl zone by the cleavelandite unit (Jahns and Ewing, 1976; Chakoumakos, 1978; Lumpkin et al., 1986). The brown thorites formed either by replacement of primary thorite or by direct precipitation from the hydrothermal fluid. We have not found much evidence in support of the first hypothesis. Primary thorite has not been found in unreplaced parts of the beryl zone, and relict cores similar in composition to thorite from the other primary lithologic units have not been observed. The second hypothesis is consistent with petrographic and chemical data presented in preceding sections of this paper. Brown thorites probably crystallized initially with compositions of approximately 50 mol% $ThSiO_4$, 40 mol% $CaTh(B^{5+}O_4)_2$, and 10 mol% $A^{3+}B^{5+}O_4$ components, where A^{3+} = Y, REEs, and Bi, and B^{5+} = P and V.

In contrast to thorite from the cleavelandite unit, the petrographic and chemical characteristics of samples from the microcline-spodumene zone reflect alteration of primary thorite during albitization of this unit. Compositions range from near–end member $ThSiO_4$ to a variety

TABLE 5. Lattice parameters of thorites from the Harding pegmatite and for synthetic compounds with the zircon structure type

	HT3		HT4		HT5	
	Unheated	Heated	Unheated	Heated	Unheated	Heated
a (Å)	7.100(7)	7.099(1)	7.150(5)	7.155(1)	7.189(2)	7.1517(9)
c (Å)	6.311(8)	6.305(1)	6.285(9)	6.340(1)	6.330(3)	6.3360(7)
V (Å³)	318.1(8)	317.7(1)	321.4(5)	324.6(1)	327.2(2)	324.08(8)
	$ThSiO_4$	$USiO_4$	$BiVO_4$	YVO_4	YPO_4	$YAsO_4$
a (Å)	7.133	6.994	7.303	7.119	6.904	7.053
c (Å)	6.319	6.263	6.458	6.290	6.033	6.285
V (Å³)	321.5	306.4	344.4	318.8	287.6	312.6

with approximately 40 mol% $ThSiO_4$ and 60 mol% $CaTh(B^{5+}O_4)_2$. The hydrothermal fluid attending albitization of the beryl zone and microcline-spodumene zone was probably enriched in Ca, V, P, Y, REEs, and Bi. U was probably depleted by earlier formation of primary U-rich thorite and microlite in the quartz zone, quartz–lath spodumene zone, and microcline-spodumene zone (cf. Lumpkin et al., 1986). Remaining U appears to have been preferentially incorporated by microlite in the cleavelandite unit. Conversely, thorite concentrated Y, REEs, and Bi relative to microlite.

Another mineral important in the partitioning of rare elements in the Harding pegmatite is zircon. Electron-microprobe analyses (Table 6) of zircons from the quartz–lath spodumene zone, microcline-spodumene zone, and cleavelandite unit suggest that zircon will incorporate very little P, U, Th, Y, and REEs in the presence of thorite and microlite. Amounts of UO_2, ThO_2, and CaO above 0.2–0.3 wt% are unusual, occurring rarely in isolated spots of a few zircon crystals. On the other hand, HfO_2 contents of zircons range from 8 to 25 wt%, typically enriched in crystal rims.

Because 10–20 m.y. are required to reach the saturation dose of $\sim 1 \times 10^{16}$ α/mg, the Harding thorites were probably still crystalline during the period of hydrothermal exchange and alteration. The alteration process began immediately after crystallization and proceeded throughout the formation of the primary zones and subsolidus replacement units. Therefore, instability introduced by radiation damage was probably not a factor in promoting primary (hydrothermal) alteration of thorite. However, sufficient damage accumulated during the period of uplift and erosion so that secondary alteration (weathering) may have been promoted by the metastable nature of the metamict state (Ewing and Haaker, 1980). It is possible that some hydration of thorite occurred in response to the accumulated alpha-recoil damage (Aines and Rossman, 1986).

The hydrous component in thorite

Thermogravimetric analyses of zircon and thorite exhibit water losses ranging from 0 to 12 wt% over a temperature interval of 150 to 600 °C. Generally, the amount of water released correlates with the extent of alpha-decay

TABLE 6. Microprobe analyses and formulas of zircons from the Harding pegmatite

	P19.1			P15.1			HT6			HT7		
P_2O_5	0.02	0.04	0.05	0.06	0.03	0.06	0.07	0.07	0.10	0.00	0.00	0.00
SiO_2	30.0	30.5	30.0	30.5	31.2	30.6	29.6	30.7	30.1	30.6	31.1	29.2
ZrO_2	56.0	56.9	55.9	55.5	57.4	55.7	47.3	55.2	52.7	53.4	52.3	51.1
HfO_2	13.5	9.98	9.63	12.1	9.75	9.28	22.7	11.5	11.3	16.4	15.1	14.3
ThO_2	0.00	0.02	0.00	0.14	0.60	0.47	0.09	1.51	3.62	0.00	0.95	4.57
UO_2	0.03	0.46	0.99	0.07	0.06	0.69	0.00	0.15	0.36	0.10	0.09	0.10
Y_2O_3	0.00	0.00	0.00	0.00	0.08	0.00	0.00	0.00	0.00	0.00	0.00	0.00
REE_2O_3	0.10	0.09	0.10	0.05	0.06	0.15	0.00	0.00	0.00	0.00	0.05	0.07
CaO	0.00	0.74	1.02	0.10	0.11	0.96	0.02	0.28	0.89	0.00	0.34	0.41
Total	99.65	98.73	97.69	98.52	99.29	97.91	99.78	99.41	99.07	100.50	99.93	99.75
Structural formulas based on O = 4.00												
P	0.001	0.001	0.002	0.002	0.001	0.002	0.002	0.002	0.003	0.000	0.00	0.000
Si	0.975	0.984	0.981	0.991	0.996	0.993	0.990	0.992	0.989	0.991	1.007	0.975
ΣB	0.976	0.985	0.983	0.993	0.997	0.995	0.992	0.994	0.992	0.991	1.007	0.975
Zr	0.896	0.904	0.900	0.889	0.907	0.892	0.780	0.881	0.855	0.854	0.837	0.843
Hf	0.125	0.091	0.090	0.113	0.090	0.086	0.218	0.107	0.108	0.153	0.141	0.138
Th	0.000	0.000	0.000	0.001	0.004	0.003	0.001	0.011	0.027	0.000	0.007	0.035
U	0.000	0.003	0.007	0.000	0.000	0.005	0.000	0.001	0.003	0.001	0.001	0.001
Y	0.000	0.000	0.000	0.000	0.001	0.000	0.000	0.000	0.000	0.000	0.000	0.000
REEs	0.001	0.001	0.001	0.001	0.001	0.002	0.000	0.000	0.000	0.000	0.001	0.001
Ca	0.000	0.024	0.036	0.003	0.004	0.033	0.000	0.010	0.031	0.000	0.012	0.015
ΣA	1.022	1.023	1.034	1.007	1.007	1.021	0.999	1.010	1.024	1.008	0.999	1.033

Note: Sample P19.1 is from the cleavelandite unit, P15.1 and HT6 are from the microcline-spodumene zone, and HT7 is from the quartz–lath spodumene zone.

damage in the crystal. Mumpton and Roy (1961) showed that compositions of thorite and zircon samples fall along the ABO_4-H_2O join and not along the ABO_4-$A(OH)_4$ join when plotted on an A-B-H_2O triangular diagram. From this, they concluded that water in natural zircon structures did not occur via the substitution of $4H^+$ for Si^{4+}, as suggested by Frondel (1953). They further stated that water in natural zircon and thorite is present as molecular water and not hydroxyl. However, reconsidering their data (Fig. 2 in Mumpton and Roy, 1961) along with ours (Fig. 6), the substitution of $4H^+$ for Si^{4+} cannot be completely ruled out because most of the data points actually fall between the two joins.

Aines and Rossman (1985, 1986) studied radiation-damaged zircons from Sri Lanka by infrared spectroscopy and concluded that the hydrous component occurs as hydroxyl groups (e.g., SiOH, ZrOH) to charge-balance damaged areas of the structure. This is consistent with plots like Figure 6. The extent of alpha-decay damage in the zircons studied by Aines and Rossman (1985, 1986) cannot be assessed because doses were not reported. In our samples of thorite, which have clearly accumulated doses well in excess of the saturation dose, molecular water is present along with hydroxyl species. We suggest that at low doses, hydroxylated A and B cations predominate, but with increased radiation damage, incorporation of molecular water becomes predominant.

Radiation effects

Calculated doses (4–12 $\times$ 10^{17} α/mg) of thorites from the Harding pegmatite are similar to extreme values experienced by U-rich microlites from the microcline-spodumene zone (Lumpkin et al., 1986). For both pyrochlore and zircon structure types at these alpha-decay doses we expect the structure to be X-ray and electron diffraction amorphous. Zircons from Sri Lanka, for example, have a well-defined saturation dose of 0.5–1.0 $\times$ 10^{16} α/mg (Holland and Gottfried, 1955; Murakami et al., 1986), corresponding to 0.4–0.8 dpa. Completely metamict thorite described by Foord et al. (1985) has a well-defined age of 6–7 m.y., from which we estimate a dose of 0.8 $\times$ 10^{16} α/mg, in agreement with the Sri Lanka zircons. Assuming a maximum saturation dose of 1 $\times$ 10^{16} α/mg, U-rich microlites and all of the thorites from the Harding pegmatite should in fact be fully metamict. This is indeed true for U-rich microlite (Lumpkin and Ewing, 1986; Lumpkin et al., 1986); however, the thorites still exhibit substantial crystallinity (see Figs. 1 and 10).

Considering the similar doses and cooling histories of the U-rich microlite and thorite, the difference may be due to the difference in chemistry. Retention of alpha-recoil damage in a crystal depends on the energy barrier to recrystallization. If this barrier is low enough, alpha-recoil damage is annealed as it accumulates. For minerals with similar temperatures of formation, the bond energies of the network-forming cation–oxygen bonds must determine in part the magnitude of this energy barrier. On a gross scale, we can compare bond energies of Ta–O for microlite and Si–O, P–O, and V–O for thorite. Reasonable values for these bond energies are available only for diatomic molecules: Ta–O, 805; Si–O, 809; P–O, 596; and V–O, 623 kJ/mol (Weast, 1985). Bond energies for P–O and V–O are roughly 200 kJ/mol lower than for Ta–O and Si–O. This supports the proposal that thorites rich in P and V have a lower energy barrier to recrystallization than either microlite or thorites that are close in composition to $ThSiO_4$. A similar conclusion has been made by Boatner and Sales (1988) for radiation damage in zircon- and monazite-type orthophosphates as compared to the orthosilicates. Additional evidence for this lies in the observation that V-rich and P-rich rims of thorite crystals tend to be more highly crystalline than Si-rich cores. Moreover, no monazites or xenotimes have ever been found to be X-ray or electron diffraction amorphous; they always retain good crystallinity despite large alpha-recoil doses (Ewing and Haaker, 1980).

Primary thorites from the quartz zone are also partially crystalline. The slope of the U-Pb correlation line in Figure 8 can be used to estimate a "recrystallization" age assuming that the amount of additional Pb above the 1:1 line is entirely radiogenic in origin. The U-Th-Pb age consistent with the U-Pb correlation line in Figure 8 is approximately 200–300 m.y. Brown thorites from the cleavelandite unit give a similar age of 100–200 m.y. based on the contents of U, Th, and Pb. If recrystallization occurred as a single event in this time frame, all of the thorites should in fact be metamict because only 10–20 m.y. are required to reach the saturation dose of 1 $\times$ 10^{16} α/mg. A more reasonable interpretation is that recrystallization is an ongoing, low-temperature process accompanied by radiogenic Pb loss. Brown P-rich and V-rich thorites have lost approximately 80% of their radiogenic Pb over 1300 m.y. In contrast, yellow thorite from the quartz zone has retained a large fraction of radiogenic Pb as $PbU(SiO_4)_2$ during recrystallization. The magnitude of Pb loss in thorites is thus controlled in part by composition and oxidation state.

Acknowledgments

We are indebted to Art Montgomery for his generous donation of the Harding pegmatite property to the University of New Mexico (UNM), for providing some of the samples for this study, and for his continued interest in pegmatite research. We are also grateful to UNM for providing funds for research and preservation of the Harding pegmatite. Arthur Russell provided assistance with the infrared spectroscopy, Elaine Faust drafted the figures, and R. C. Ewing reviewed an early version of the manuscript. We also appreciate the constructive reviews of J. A. Speer and George Robinson. Purchase of the FT-IR spectrometer was facilitated by NSF grant CHE-80007979 to the Department of Chemistry, UNM. Electron-microprobe analyses and transmission electron microscopy were completed in the Electron Microbeam Analysis Facility in the Department of Geology and Insititute of Meteoritics at UNM, supported in part by NSF, NASA, DOE-BES, and the State of New Mexico. This work was supported by the Department of Energy, Office of Basic Energy Sciences, under grant DE-FG04-84ER45099 (R. C. Ewing, principal investigator).

REFERENCES CITED

Aines, R.D., and Rossman, G.R. (1985) The high temperature behavior of trace hydrous components in silicate minerals. American Mineralogist, 70, 1169–1179.

——— (1986) Relationships between radiation damage and trace water in zircon, quartz, and topaz. American Mineralogist, 71, 1186–1193.

Albee, A.L., and Ray, L. (1970) Correction factors for electron probe microanalysis of silicates, oxides, carbonates, phosphates and sulfates. Analytical Chemistry, 42, 1408–1414.

Aldred, A.T. (1984) Crystal chemistry of ABO_4 compounds. In G.S. Barney, J.D. Navrital, and W.W. Schultz, Eds., Geochemical behavior of disposed radioactive waste, ACS Symposium Series, vol. 246, p. 305–314. American Chemical Society, Columbus, Ohio.

Åmli, R. (1975) Mineralogy and rare earth geochemistry of apatite and xenotime from the Gloserheia granite pegmatite, Froland, southern Norway. American Mineralogist, 60, 607–620.

Appleman, D.E., and Evans, H.T., Jr. (1973) Indexing and least-squares refinement of powder diffraction data. U.S. National Technical Information Service, Document PB-216-188.

Bence, A.E., and Albee, A.L. (1968) Empirical correction factors for the electron microanalysis of silicates and oxides. Journal of Geology, 76, 382–403.

Boatner, L.A., and Sales, B.C. (1988) Monazite ceramic nuclear waste forms. In R.C. Ewing and W. Lutze, Eds., Radioactive waste forms for the future. North-Holland, Amsterdam, in press.

Brookins, D.G., Chakoumakos, B.C., Cook, C.W., Ewing, R.C., Landis, G.P., and Register, M.E. (1979) The Harding pegmatite: Summary of recent research. In R.V. Ingersoll and L.A. Woodward, Eds., New Mexico Geological Society Guidebook, 30th Field Conference, 127–133.

Chakoumakos, B.C. (1978) Microlite, the Harding pegmatite, Taos County, New Mexico. B.S. thesis, University of New Mexico, Albuquerque, New Mexico.

Dreyer, G., and Tillmanns, E. (1981) Dreyerite, natural tetragonal bismuth vanadate from Hirschhorn, Pfalz. Neues Jahrbuch für Minealogie Monatshefte, 151–154 (in German) [abs. translated in American Mineralogist, 67, 622 (1982)].

Ewing, R.C. (1974) Spherulitic recrystallization of metamict polycrase. Science, 184, 561–562.

——— (1975) The crystal chemistry of complex niobium and tantalum oxides. IV. The metamict state: Discussion. American Mineralogist, 60, 728–733.

Ewing, R.C., and Haaker, R.F. (1980) The metamict state: Implications for radiation damage in crytalline waste forms. Nuclear and Chemical Waste Management, 1, 51–57.

Foord, E.E., Cobban, R.R., and Brownfield, I.K. (1985) Uranoan thorite in lithophysal rhyolite—Topaz Mountain, Utah, USA. Mineralogical Magazine, 49, 729–731.

Frondel, C. (1953) Hydroxyl substitution in thorite and zircon. American Mineralogist, 38, 1007–1018.

——— (1958) Systematic mineralogy of uranium and thorium. U.S. Geological Survey Bulletin 1064, 400 p.

Heinrich, E.W. (1963) Xenotime and thorite from Nigeria. American Mineralogist, 48, 206–208.

Hirschi, H. (1928) Thormineral aus lithiumpegmatit von camp Harding bei Embudo, New Mexico. Schweizerische Mineralogische und Petrographische Mitteilungen, 8, 260–261.

Hogarth, D.D., and Miles, N.M. (1969) Wakefieldite, natural YVO_4 (abs.). Canadian Mineralogist, 10, 136–137.

Holland, H.D., and Gottfried, D. (1955) The effect of nuclear radiation on the structure of zircon. Acta Crystallographica, 8, 291–300.

Hutton, C.O. (1950) Heavy detrital minerals. Geological Society of America Bulletin, 61, 635–710.

Jahns, R.H., and Ewing, R.C. (1976) The Harding mine, Taos County, New Mexico. In R.C. Ewing and B.S. Kues, Eds., New Mexico Geological Society Guidebook, 27th Field Conference, 263–276.

——— (1977) The Harding mine, Taos County, New Mexico. Mineralogical Record, 8, 115–126.

Kim, S.J. (1978) Chemical composition of coffinite from the Woodrow mine, New Mexico, U.S.A. Mining Geology (Korea), 11, 183–186.

Lumpkin, G.R., and Chakoumakos, B.C. (1986) Thorite group minerals from the Harding mine, Taos County, New Mexico (abs.). Geological Association of Canada–Mineralogical Association of Canada Joint Annual Meeting, 11, 96–97.

Lumpkin, G.R., and Ewing, R.C. (1986) High resolution transmission electron microscopy of microlite from the Harding pegmatite, Taos County, New Mexico. In A.D. Romig, Jr., and W.F. Chambers, Eds., Microbeam analysis—1986, p. 145–147. San Francisco Press, San Francisco.

Lumpkin, G.R., Chakoumakos, B.C., and Ewing, R.C. (1986) Mineralogy and radiation effects of microlite from the Harding pegmatite, Taos County, New Mexico. American Mineralogist, 71, 569–588.

Miles, N.M., Hogarth, D.D., and Russell, D.S. (1971) Wakefieldite, yttrium vanadate, a new mineral from Quebec. American Mineralogist, 56, 395–410.

Mitchell, R.S. (1973) Metamict minerals: A review. Mineralogical Record, 4, 214–223.

Muller, O., and Roy, R. (1974) The major ternary structural families, 487 p. Springer-Verlag, New York.

Mumpton, F.A., and Roy, R. (1961) Hydrothermal stability studies of the zircon-thorite group. Geochimica et Cosmochimica Acta, 21, 217–238.

Murakami, T., Chakoumakos, B.C., and Ewing, R.C. (1986) X-ray powder diffraction analysis of alpha-event radiation damage in zircon ($ZrSiO_4$). In D.E. Clark, W.B. White, and J. Machiels, Eds., Nuclear waste management II, Advances in ceramics, vol. 20, p. 745–753. American Ceramic Society, Columbus, Ohio.

Northrop, S.A. (1959) Minerals of New Mexico (revised edition). University of New Mexico Press, Albuquerque.

Pabst, A. (1952) The metamict state. American Mineralogist, 37, 137–157.

Pabst, A., and Hutton, C.O. (1951) Huttonite, a new monoclinic thorium silicate; with an account of its occurrence, analysis and properties. American Mineralogist, 36, 60–69.

Palache, C., Berman, H. and Frondel, C. (1944) Dana's system of mineralogy, vol. 1 (7th edition). Wiley, New York.

Robinson, S.C., and Abbey, S. (1957) Uranothorite from eastern Ontario. Canadian Mineralogist, 6, 1–15.

Rose, D. (1980) Brabantite, $CaTh(PO_4)_2$, a new mineral of the monazite group. Neues Jahrbuch für Mineralogie Monatshefte, 247–257.

Speer, J.A. (1982) The actinide orthosilicates. Mineralogical Society of America Reviews in Mineralogy, 5, 113–135.

Staatz, M.H., Adams, J.W., and Wahlberg, J.S. (1976) Brown, yellow, orange, and greenish-black thorites from the Seerie Pegmatite, Colorado. U.S. Geological Survey Journal of Research, 4, 575–582.

Taylor, M., and Ewing, R.C. (1978) The crystal structures of the $ThSiO_4$ polymorphs: Huttonite and thorite. Acta Crystallographica, B34, 1074–1079.

Weast, R.C. (1985) CRC handbook of chemistry and physics. CRC Press, Cleveland.

MANUSCRIPT RECEIVED NOVEMBER 30, 1987
MANUSCRIPT ACCEPTED AUGUST 1, 1988